Dynamics and Relative Stabilities of Parallel- and Antiparallel-Stranded DNA Duplexes

Angel E. Garcia,* Dikeos M. Soumpasis,‡ and Thomas M. Jovin‡

*Theoretical Biology and Biophysics Group, Los Alamos National Laboratory, Los Alamos, New Mexico 87545 USA, and ‡Department of Molecular Biology, Max Planck Institute for Biophysical Chemistry, 37078 Goettingen, Germany

ABSTRACT The dynamics and stability of four DNA duplexes are studied by means of molecular dynamics simulations. The four molecules studied are combinations of 4, 15 bases long, single-stranded oligomers, F1, F2, F3, and F4. The sequence of these single strand oligomers are chosen such that F1-F2 and F3-F4 form parallel (ps) DNA double helices, whereas F1-F4 and F2-F3 form antiparallel-stranded (aps) DNA double helices. Simulations were done at low (100 K) and room (300 K) temperatures. At low temperatures the dynamics are quasi-harmonic and the analysis of the trajectories gives good estimates of the low frequency vibrational modes and density of states. These are used to estimate the linear (harmonic) contribution of local fluctuations to the configurational entropy of the systems. Estimates of the differences in enthalpy between ps and aps duplexes show that aps double helices are more stable than the corresponding ps duplexes, in agreement with experiments. At higher temperatures, the distribution of the fluctuations around the average structures are multimodal and estimates of the configurational entropy cannot be obtained. The multi-basin, nonlinear character of the dynamics at 300 K is established using a novel method which extracts large amplitude nonlinear motions from the molecular dynamics trajectories. Our analysis shows that both ps DNA exhibit much larger fluctuations than the two aps DNA. The large fluctuations of ps DNA are explained in terms of correlated transitions in the β, ϵ, and ζ backbone dihedral angles.

INTRODUCTION

Double-stranded parallel DNA with reverse Watson-Crick base pairing have been the subject of experimental studies for the past five years. These studies were originally motivated by the theoretical modeling work of Pattabiraman (1986), which showed that parallel DNA could be energetically favored over the conventional antiparallel DNA. The first structural and thermodynamic studies of parallel-stranded DNA were done on a chemically modified hairpin sequence, $dA_{10}C_4T_{10}$, in which two arms of the hairpin stem run parallel to each other (van de Sande, 1988). Subsequently, other sequences were chosen in such a way that the parallel-stranded DNA (ps-DNA), right-handed double helices were energetically more favorable than the regular antiparallel-stranded DNA (aps-DNA) (Ramsing, 1988, 1989; Rippe, 1989a, b). These sequences were 15 nucleotide (NT) long (labeled as the *F-series* by Ramsing et al., 1988) and 25 NT long (labeled as a *D-series*). Most of the sequences studied are mainly composed of Adenine-Thymine exhibiting reverse Watson-Crick base pairing and with the glycosidic bonds in the *trans* orientation. A reverse Watson-Crick base pairing is formed by hydrogen bonds between N6 of Adenine (A) and O2 of Thymine (T), and the usual hydrogen bond between N3 of A and N1 of T. Ab Initio quantum chemical calculations (Hobza, 1987) predict equal stability for either WC of reverse WC base pairing. Other base pairings patterns in a *trans* orientation (i.e., parallel helices) with at least two hydrogen bonds have been theoretically analyzed (Il'lichova, 1990).

Under physiological conditions, ps-DNA is the most stable alternative to the regular aps B DNA structures known to date. For example, the differences in enthalpy in the helix-coil transition is 5 ± 0.5 Kcal/mol for ps-DNA, and 6 ± 0.5 Kcal/mol for aps-DNA in NaCl. The melting temperature of ps-DNA are 13–19°C lower than for similar aps-DNA sequences (German, 1988; Ramsing, 1988; Jovin, 1990; Rippe, 1989a, b; Rentzeperis, 1992). ^{1}H NMR and ^{31}P NMR studies (Germann, 1989) show that ps-DNA exhibit large backbone flexibility. A large number of P NMR resonances suggest that many ϵ and β dihedral angles can be sampled by the backbone (Powers, 1989, 1990; Lankhorst, 1984). 2D NMR of the $dA_{10}C_4T_{10}$ (van de Sande, 1988) hairpin has recently been reported (Zhow, 1993). The sugar and glycosidic angle conformations are those of B-DNA.

Other sequences containing different base pairings have been recently reported (Rippe, 1992a; Robinson, 1992, 1993). Rippe et al. (1992a) have found that alternating $(GpA)_n$ self associates, under physiological conditions, into stable double-helical structures. Fluorescence studies of oligonucleotides end-labeled with pyrene showed that the double helices are parallel-stranded. In addition, physicochemical studies, and previous thermodynamics studies (Lee, 1979, 1980, 1990) indicated that A.A and G.G base pairs are formed. These ps-DNA with polypurine sequences can play a role in recombination, gene expression, and in the stabilization of the genomic structure. For example, 0.4% of the total genome is constituted by $d(GpA)_{n>20}$. These sequences are very common in centromeric regions of the human genome chromosomes (Grady, 1992; Catasti, 1994).

Received for publication 29 October 1993 and in final form 17 March 1994.

Address reprint requests to Angel E. Garcia, Theoretical Biology & Biophysics Group, T-10, Mail Stop K710, Los Alamos National Laboratory, Los Alamos, NM 87545. Tel.: 505-665-5341; Fax: 505-665-3493; E-mail: angel@t10.lanl.gov.

0006-3495/94/06/1742/14 $2.00

In this work we describe the dynamics and stability of four DNA oligomers by means of molecular dynamics simulations and normal mode analysis.

The four molecules studied are four duplexes (2 ps and 2 aps) formed by combining four 15 nt long, single-stranded oligomers studied by Rippe et al. (1989a, b). The sequences of these oligomers were chosen such that F1-F2 and F3-F4 form parallel-stranded (ps) DNA double helices, whereas F1-F4 and F2-F3 form antiparallel-stranded (aps) DNA double helices. Thermodynamic data are available for two of these duplexes, F1-F2 (ps) and F3-F4 (aps).

DESCRIPTION OF THE SYSTEM

The four 15-mers studied are constructed from the sequences

F1: *TTTTTATTAAATATA*
F2: *AAAAATAATTTATAT*
F3: *ATATAAATTATTTTT*
F4: *TATATTTAATAAAAA*.

The combinations of these single strands form the following DNA double helices:

1. F1.F2 ps DNA.
2. F3.F4 *ps* DNA.
3. F1.F4 *aps* DNA.
4. F2.F3 *aps* DNA.

Each oligomer forms part of one aps and ps DNA molecule. By analyzing the dynamics of the four double helices described above, we can compare the conformation, dynamics (in terms of fluctuations), and energetics of the four oligomers F1, F2, F3, and F4 when forming part of ps and aps duplexes. The starting configurations used in the molecular dynamics simulations were constructed by generating four B-DNA single helices with the sequences in F1, F2, F3, and F4. Each single helix was formed starting from Arnott's ideal B-DNA conformation (Arnott, 1979). The aps DNA double helices were formed in the usual way by imposing a pseudo twofold symmetry about the bases major axis. The ps strand was formed by rotating the complementary strand by 180° around the helix axis (Pattabiraman, 1986; Zhow, 1993). The resulting double helices form Watson-Crick A-T base pairs in aps DNAs, and a reverse Watson-Crick A-T base pairs in ps-DNA.

COMPUTATIONAL METHODS

Energy minimization and molecular dynamics

Each of the four duplexes consists of 958 atoms, including hydrogens. Energy calculations were done using the *All-atoms* force field of Weiner et al. (1986). All calculations were done in vacuo using AMBER 4.0 (Pearlman, 1991). The Coulomb energy terms were screened with a dielectric coefficient of 78.5 to emulate the dielectric screening properties of bulk water. A residue-base cutoff of 12.5 Å was used for all nonbonding interactions. The initial structures were subjected to energy minimization for 5000 steps. At the end of the minimizations, the resulting structures were used as starting conformations for the MD simulations. During the MD simulations, the ends base pairs of each molecule were constrained to the energy minimized positions to avoid fraying of the end base pairs of the system and to constrain the configurational sampling to double-helical conformations. The remaining 13 base pairs of each duplex were allowed to sample conformations during the MD simulation.

Molecular dynamics simulations were done at two temperatures (100 and 300 K) by weakly coupling the system to an external bath (Berendsen et al., 1984). Each system was heated to 300 K during the first 5 ps of simulation. An integration time step of 0.001 ps was used during the heating period. After the first 5 ps, the Newton's equations of motion for the systems were integrated for a period of 200 ps (each) without any rescaling or further intervention. The integration step was 0.002 ps. Heavy-atom to hydrogen atom bond lengths were constrained using SHAKE (van Gunsteren et al., 1977) (with a tolerance of 0.0005 Å). During all MD simulations, the hydrogen bonds between base pairs were constrained with a step potential, which is zero for hydrogen, to acceptor distances between 1.8 and 2.2 Å and have a quadratic energy penalty function (35 Kcal/mol Å^2) for distances outside this range. These constraints limit the configurational sampling to regions with the desired base pairings. No angular constraints between donor-hydrogen-acceptor triplets were imposed. After the first 205 ps of simulations, the systems were cooled to 100 K during a period of 10 ps. Additional simulations of 150 ps (using a 0.001 ps integration step) were done at 100 K for all four duplexes. Configurations were saved every 0.1 ps. These configurations were subjected to the analyses described below.

Analysis of the MD trajectories

The trajectories generated via the MD simulations contain a wealth of important hidden information that can only be extracted via special techniques of data analysis. Such a technique has been previously introduced and briefly described (Garcia, 1992) to establish the nature of the conformational space sampling (one basin of attraction, quasi-harmonic motion versus multiple basins, nonlinear motions) performed during the MD simulation of a protein in solution. This technique is used here, too, and will be described next in greater detail because, in general, it is a valuable tool for the quantitative analysis of biomolecular dynamics.

The method involves the construction of a set of directions $\vec{m}^{3N}$ in the 3N dimensional conformational space, which can be most efficiently used to describe the structural fluctuations of the molecule under study.

The directions $\vec{m}^{3N}$ are determined by minimizing the mean-square distances of the $\{\vec{r}_i^{3N}\}$ configurations *normal* to $\vec{m}^{3N}$, such that most of the fluctuations will be along $\vec{m}^{3N}$. (We refer to Fig. 1 for a graphical definition of terms used in the following mathematical derivations.) The distance between a point $\vec{r}_i$, which here represents a biomolecule conformation, and a line with direction $\vec{m}$, passing through the point $\vec{y}_0$, is given by

$$d_i^2 = (\vec{r}_i - \vec{y}_0)^2 - [(\vec{r}_i - \vec{y}_0) \cdot \vec{m}]^2.$$

The average square distance between a set of L points representing all the trajectory points of the biomolecule is then given by

$$d^2 = \frac{1}{L}\sum_{i=1}^{L} d_i^2 = \frac{1}{L}\sum_{i=1}^{L} (\vec{r}_i - \vec{y}_0)^2 - [(\vec{r}_i - \vec{y}_0) \cdot \vec{m}]^2. \quad (1)$$

The least-square distance is obtained by finding the 6N parameters $\vec{y}_0 = \{y_{0\alpha}\}$ and $\vec{m} = \{m_\alpha\}$, with $\vec{m} \cdot \vec{m} = 1$, that minimize d^2. That is, we have to minimize a function of the trajectories, $x_i(t)$, and a function of $\vec{m}$, $\vec{y}_0$, and λ

$$f(\vec{m}, \vec{y}_0, \lambda) = \frac{1}{L}\sum_{i=1}^{L} \{(\vec{r}_i - \vec{y}_0)^2 - [(\vec{r}_i - \vec{y}_0) \cdot \vec{m}]^2\} + \lambda[\vec{m} \cdot \vec{m} - 1], \quad (2)$$

where λ is a Lagrange multiplier. An extreme value of d^2 is given by a set $\vec{z} = (m_\alpha, y_{0,\alpha}, \alpha = 1, \cdots, 3N, \lambda)$, which gives $\nabla_{\vec{z}} f(\vec{z}) = 0$. The gradient of $f(\vec{m}, \vec{y}_0, \lambda)$ gives,

i) with respect to $\vec{y}_0$,

$$\nabla_{\vec{y}_0} f = \frac{2}{L}\sum_{i=1}^{L} \{-(\vec{r}_i - \vec{y}_0) + [(\vec{r}_i - \vec{y}_0) \cdot \vec{m}]\vec{m}\} = 0, \quad (3)$$

which implies

$$\vec{y}_0 = \frac{1}{L}\sum_{i=1}^{L}\vec{r}_i. \tag{4}$$

That is, $\vec{y}_0$ is the average over all configurations;

ii) with respect to λ,

$$\nabla_\lambda f = \vec{m}\cdot\vec{m} - 1 = 0, \tag{5}$$

which normalizes the vector $\vec{m}$;

iii) with respect to m_α,

$$\nabla_{m_\alpha} f = -\frac{1}{L}\sum_{i=1}^{L}\{(r_i - y_0)_\alpha (r_i - y_0)\cdot\vec{m}\} + \lambda m_\alpha = 0. \tag{6}$$

We can rewrite the right-hand side of Eq. 6 as

$$\frac{1}{L}\sum_{\beta=1}^{3N}\sum_{i=1}^{L}(r_i - y_0)_\alpha (r_i - y_0)_\beta m_\beta = \lambda m_\alpha. \tag{7}$$

Defining

$$\sigma_{\alpha,\beta} = \frac{1}{L}\sum_{i=1}^{L}(r_i - y_0)_\alpha (r_i - y_0)_\beta, \tag{8}$$

where $\sigma_{\alpha,\beta}$ is positive semi-definite, we obtain

$$\sigma\cdot\vec{m} = \lambda\vec{m}, \tag{9}$$

which is the eigenvalue equation for σ. σ has 3N eigenvalues, λ_α, and 3N eigenvectors, $\vec{m}_\alpha$.

To find out which eigenvectors $\vec{m}_\alpha$ minimize d^2, we evaluate d^2 for each line defined by the direction $\vec{m}_\alpha$ and $\vec{y}_0$. That is,

$$\begin{aligned} d^2(\vec{m}_\alpha) &= \frac{1}{L}\sum_{i=1}^{L} d_i^2 = \frac{1}{L}\sum_{i=1}^{L}(r_i - y_0)^2 - [(r_i - y_0)\cdot\vec{m}_\alpha]^2 \\ &= \frac{1}{L}\sum_{i=1}^{L}\left[\left(\sum_{\mu=1}^{3N}(r_i - y_0)_\mu^2\right) - \sum_{\mu=1,\nu=1}^{3N}(r_i - y_0)_\mu (r_i - y_0)_\nu m_{\alpha,\mu} m_{\alpha,\nu}\right] \\ &= \mathrm{Tr}(\sigma) - \vec{m}_\alpha\cdot\sigma\cdot\vec{m}_\alpha. \end{aligned} \tag{10}$$

The eigenvector corresponding to the largest eigenvalue corresponds to the direction of the line passing through the average conformation, $\vec{y}_0$, which best represents the predominant motions of the DNA duplexes.

Notice that Eqs. 8 and 9 are closely related to the definitions used in the quasi-harmonic approximation (Karplus, 1981; Levy, 1984; Brooks, 1988). In the quasi-harmonic approximation, the eigenvalue system solved involves the matrix

$$K_{\mu\nu} = kT\sqrt{a_\mu a_\nu}\,\sigma^{-1}_{\mu,\nu}, \tag{11}$$

where σ is defined by Eq. 8, $\sigma^{-1}_{\mu,\nu}$ refers to an element of the inverse of the matrix σ, and a_μ is the mass of atom μ. The difference between quasi-harmonic analysis and the analysis presented here is that we do not assume unimodal distributions of the atomic fluctuations (i.e., motions in a single basin of attraction or, in other words, around a single minimal energy structure). As shown below, at room temperature the distributions of atomic fluctuations are not unimodal and, therefore, the quasi-harmonic approximation has no validity. At low temperature (100 K), the distributions of fluctuations around equilibrium are unimodal and the quasi-harmonic approximation can be correctly used to obtain estimates of the configurational contributions to the free energy of the DNA duplexes.

Eigenvectors and eigenvalues are computed from the simulation data by calculating σ in Eq. 8. Having done so, the projection of the motion $\vec{r}^{3N}(t)$ along a given eigenvector $\vec{m}_\alpha$,

$$p_\alpha(t) = \vec{r}(t)\cdot\vec{m}_\alpha, \tag{12}$$

yields a picture of the motion in a set of generalized natural coordinates for the biomolecule.

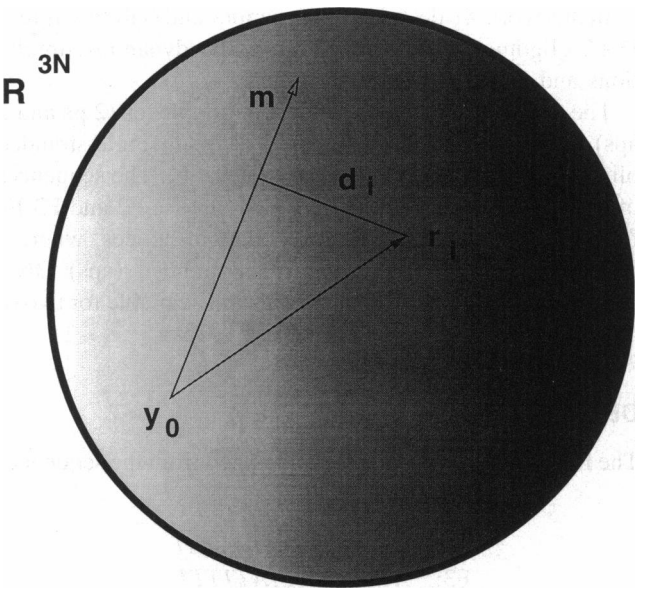

FIGURE 1 Representation of the 3N dimensional configurational space of the four DNA duplexes. The direction, $\vec{m}$, represents a unit vector in this space that best describes the fluctuations of a duplex; $\vec{y}_0$ represents the average configuration; $\vec{r}_i$ represents the configuration adopted at the *i*th time interval during the MD simulation. The distance d_i is the distance between the point $\vec{r}_i$ and the direction $\vec{m}_i$. Relations between these vectors and distances are described in Eqs. 1–10.

Analysis of dihedral angle transitions

The time history of dihedral angles about a minimum is commonly studied by means of time auto-correlation functions. This analysis is appropriate if the dynamics occur around one center, i.e., are unimodal. However, it is known (Helfand, 1983; Krumhansl, 1985; Garcia, 1992) that in polymeric systems the options of many, but not all, dihedral angles exhibit fast transitions between two or more minima and damped oscillations in between transitions. The transitions are fast, but the residence time between transitions can be long. This phenomena is responsible for most of the large atomic fluctuations in a molecule and cannot be extracted from simple auto-correlation functions. Therefore, following the formalism described by Helfand (1983), we analyze these motions by means of a methodology from reliability theory, called Hazard Analysis.

This analysis consists of studying the first passage times from one minimum to another. This analysis presumes that transition rates are only a function of the time since the last transition; that is, memory of previous transitions is neglected. In our implementation of this analysis, we study a complementary function defined by the probability of an angle to remain at a minimum well at time $t + t'$, given that it was at the same well at time t. This function is obtained by evaluating a binary time series, $A(1, \cdots, t)$, where at every time interval a *yes* or *no* question is answered. A function, $P(t = t_2 - t_1)$ gives the fraction of the time in which $t - 1$ consecutive components of A are one. Using this definition, $P(0)$ gives the fraction of the time that the discretized time series $A(t)$ gives a *yes* answer. Fitting the function $P(t)$ to a single exponential, $P(t) = P(0)\exp(-t/\tau)$, gives the time, τ, at which, on the average, $A(i)$ will be *zero* after being *one*. That is, a single exponential fitting presumes a Poisson process in which *a particle* escapes a minimum well with a *decay* time τ.

This analysis will be used here to describe the transition rates of sugar backbone dihedral angles between two (or more) local minima. One time series is kept for each minimum. For example, in studying the transition of the angle ϵ from t to g^+ and back, we define two time series, $A_{t\to g^+}$ and $A_{g^+\to t}$. The time series, $A_{t\to g^+}$, will change its value every time that ϵ crosses a minimum (t or g^+) for the first time after it crossed the other minimum (g^+ or t). We use the following definition to determine the value of the time series, A, for the first configuration: $A_{t\to g}(1) = 1$ if the value $\epsilon(1)$ is closer

to g^+ than to t, and zero otherwise. By imposing this condition, $A_{t\to g}$ is made complementary to $A_{g\to t}$. (that is, $A_{g\to t}$ and $A_{t\to g} = 0$, and $A_{g\to t}$ or $A_{t\to g} = 1$). A similar analysis is also used for studying the mean lifetime of hydrogen bonds.

RESULTS

Time histories and population distributions of the Cartesian coordinates fluctuations from the mean conformations, hydrogen bonding, and the sugar-backbone dihedral angles were calculated from the molecular dynamics trajectories at 300 K. The results of these analyses are discussed in the following subsections.

Average conformations

The average conformations and fluctuations for all four duplexes are calculated in the following way. At regular time intervals (0.1 ps) along the trajectory, a saved configuration is rotated and translated such that the distance between a reference and the saved MD configuration is minimized. These minimum distances are calculated by using the method of McLachlan (1979). The time average structures for each MD trajectory are obtained as the sum all the rotated MD conformations in 3N dimensional space. Fig. 2 shows plots of the average conformations of the four duplexes. Notice that the ps-DNA double helices have two identical grooves and that the inter-strand P to P distances are, in general larger, than those in aps-DNA. The two aps-DNA duplexes show typical minor and major grooves.

Helical parameters of all the structures were determined using the Tung Soumpasis. Examples are given in Tables 1 and 2 for a ps and aps duplex, respectively. Compared to the aps form, the ps form is characterized by somewhat larger twist and D_z values, but lower propeller twists.

The mean square displacements (MSD) during the MD simulation are calculated as the variance, $\langle x_i^2\rangle - \langle x_i\rangle^2$. If the distances are calculated using the time average conforma-

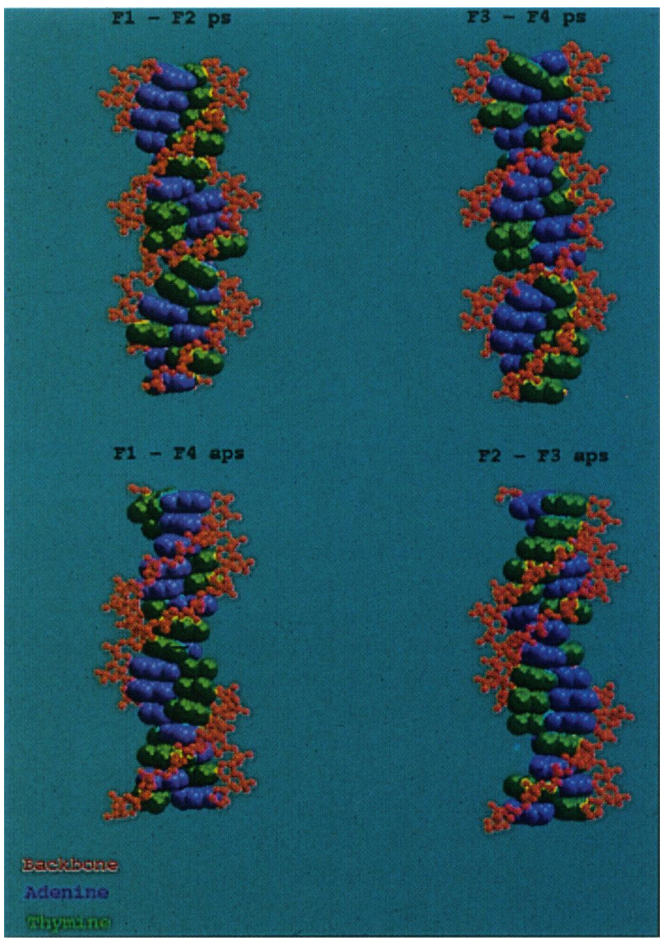

FIGURE 2 Space-filling plots of the average conformations of the four duplexes. The ps-DNA double helices have two identical grooves, and the inter-strand P to P distances are, in general larger, than those in aps-DNA. The two aps-DNA duplexes show typical minor and major grooves. The color coding is adenine (*green*), thymine (*purple*) and backbone atoms (*red*). The van der Waals radius of the backbone atoms were scaled by 0.20 of their value.

TABLE 1 Helical parameters for F2-F3 aps-DNA

Sequence	τ	Ω	ρ	dx	dy	dz	buckle	Open	Prop. Twist
30 T-1 **A**							8.9	−12.8	−23.6
29 T-2 **A**	1.2	29.6	4.1	0.32	−0.47	3.2	4.0	−10.9	−23.1
28 T-3 **A**	1.0	34.6	1.1	0.32	−0.54	3.2	4.7	−10.9	−22.1
27 T-4 **A**	0.9	35.4	−1.1	0.32	−0.64	3.2	3.4	−12.1	−22.1
26 T-5 **A**	1.7	37.6	−4.5	0.28	−0.71	3.2	3.9	−14.0	−17.7
25 A-6 **T**	0.3	26.6	−10.6	−0.28	−0.52	3.3	−1.4	−14.0	−17.0
24 T-7 **A**	1.2	46.4	7.0	0.14	−0.82	3.1	2.8	−11.7	−22.0
23 T-8 **A**	1.9	35.3	−2.5	0.22	−0.47	3.2	3.4	−13.2	−20.8
22 A-9 **T**	−0.5	27.5	−12.0	−0.21	−0.40	3.3	−6.3	−13.7	−20.5
21 A-10 **T**	−2.9	37.9	−3.5	0.03	−0.70	3.2	−10.1	−11.9	−21.5
20 A-11 **T**	−2.3	36.1	−2.3	0.02	−0.61	3.2	−10.7	−11.3	−19.3
19 T-12 **A**	0.0	48.8	4.5	0.7	−0.50	3.2	2.0	−13.5	−12.5
18 A-13 **T**	0.6	21.4	−7.0	−0.07	−0.40	3.4	2.4	−13.3	−12.3
17 T-14 **A**	2.0	48.5	10.1	0.55	−1.12	3.1	11.5	−14.1	−18.2
16 A-15 **T**	1.2	14.4	−5.8	−0.21	−0.43	3.3	3.6	−16.1	−24.5
Avg:	0.45	34.3	−1.6	0.15	−0.60	3.22	1.5	−12.9	−19.8

Obtained from the definitions of Soumpasis-Tung (1988) method. The parameters defined correspond to the angles (in degrees) τ = tilt; Ω = twist; and dx, dy, and dz describe displacements (in Å) along the major axes, minor axes, and the helix axes, respectively. The average values for each parameter are listed in the last row.

TABLE 2 Helical parameters for F1-F2 ps-DNA

Sequence	τ	Ω	ρ	dx	dy	dz	buckle	Open	ω
16 A-1 T							−21.7	161.3	15.2
17 A-2 T	−2.3	36.7	−4.0	−0.55	−0.17	3.2	−23.3	159.4	21.3
18 A-3 T	−0.6	35.1	−0.7	−0.43	0.03	3.2	−19.4	156.8	23.3
19 A-4 T	−1.3	37.9	5.1	0.28	0.00	3.2	−18.9	156.9	21.7
20 A-5 T	−1.8	37.0	3.4	0.09	0.13	3.3	−16.9	159.6	15.8
21 A-6 A	4.9	38.6	13.6	−0.16	−0.49	3.5	19.7	195.8	−13.1
22 A-7 T	−5.4	37.7	−5.1	1.11	0.83	3.3	−23.5	157.6	7.9
23 A-8 T	−3.7	37.7	−2.2	−0.27	−0.16	3.3	−25.1	159.4	14.3
24 A-9 A	3.5	32.6	12.5	−0.45	−0.75	3.4	10.1	200.3	−8.4
25 A-10 A	7.6	45.1	21.3	1.84	0.23	3.2	39.0	204.5	−18.6
26 A-11 A	1.0	35.2	−4.0	0.22	0.03	3.2	21.4	197.9	−33.5
27 A-12 T	−3.0	38.7	−9.1	0.43	0.56	3.4	−12.5	161.5	25.7
28 A-13 A	3.9	36.1	8.0	−0.66	−0.81	3.5	12.1	196.5	−17.3
29 A-14 T	−2.2	37.1	−0.12	1.30	0.81	3.3	−21.0	160.4	7.8
30 A-15 A	2.0	32.6	10.5	−0.72	−0.68	3.4	8.9	200.9	0.9
Avg:	0.2	37.0	3.5	0.15	−0.03	3.3	−4.7	175.3	4.2

Obtained from the definitions of Soumpasis-Tung (1988). All parameters are defined in the caption for Table 1.

tions as the reference structures instead of an arbitrary conformation, we would obtain identical results. The average MSD deviations from these structures are 1.7 and 1.5 Å^2 for the ps F1.F2 and F3.F4 duplexes, respectively, and 0.86 and 0.84 Å^2 for F1.F4 and F2.F3 aps duplexes, respectively. At low temperature (100 K), the MSD are similar for all four double helices (~0.30 Å^2). Fig. 3 shows the atom-by-atom MSD fluctuations for each of the four single strands in both ps and aps conformations. These MSD values correspond to the deviations of each strand when forming a double helix and are obtained while optimizing the distance from each corresponding double helix. It is found that every single-strand oligomer shows much larger fluctuations in the ps conformation than in the aps conformation.

To identify which motions are responsible for the larger fluctuations in ps duplexes, we have calculated the average and SDs of all sugar-phosphate backbone dihedral angles (Saenger, 1984) for the four oligomers, in each of the two conformations. For example, Tables 3 and 4 show average angles and their SDs for the F2 strand in a ps and aps duplex, respectively. The average sampled dihedral angles for each oligomer are similar in the ps and aps conformations, but many dihedral angles in the ps conformation show much larger SDs. In particular the sequences: ϵ_i, ζ_i, β_{i+1} of bases T_2 and T_7 of F1 (ps); A_3, A_4, T_6, A_7, T_9 and T_{13} of F2 (ps); A_3, T_4, A_5, A_6 of F3 (ps); and A_8, A_9, and A_{12} of F4 (ps). In the aps conformations, only T_8 of F1 (aps) show large SD values in ϵ and ζ. All δ dihedral angles (of each strand in ps and aps conformations) show relatively large SD values. This is indicative of sugar pucker variations during the dynamics of all oligomers.

The averages of each of the sugar backbone dihedral angles in each of the four strands in both ps and aps do not differ by more than 11° from the corresponding angles in any of the strands. The average conformation of each and every strand is a typical B-DNA helix with average angles (in degrees, with the minimum and maximum values between parenthesis): α = 292 (292–293); β = 170 (166–173); γ = 63 (62–63); δ = 118 (114–120); ϵ = 183 (179–189); ζ = 263 (254–265); and χ = 239 (234–244). A survey of the reported x-ray structures classified as B-DNA double helices

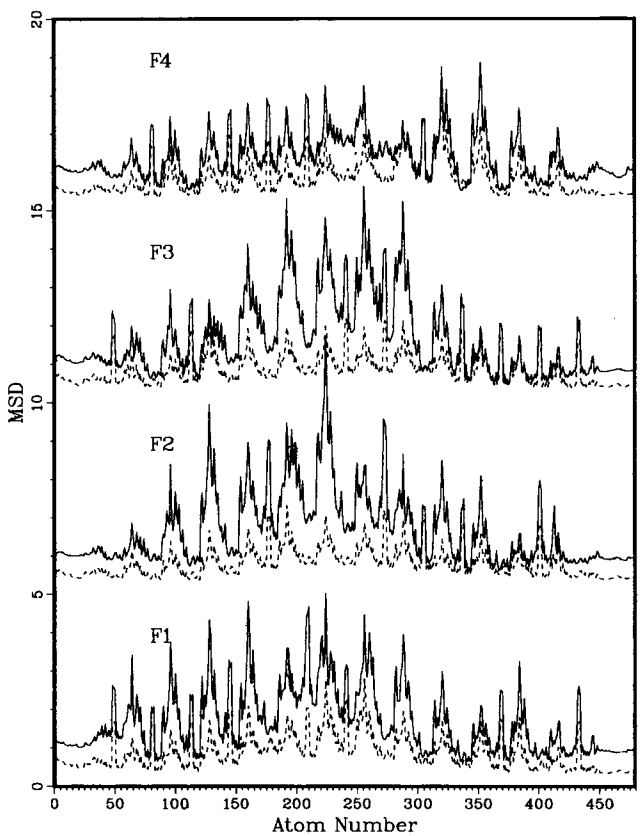

FIGURE 3 Mean square displacements (MSD), in Å^2, for the four single stranded oligomers, F1, F2, F3, and F4, during MD trajectories (at 300K) in the ps and aps double helices. The curves for oligomers F2, F3, and F4 were displaced by 5, 10, and 15 Å^2, respectively. For each set of curves, the top curve (showing the largest MSD) corresponds to the atomic ms fluctuations when in the ps conformations, whereas the lower curves corresponds to the ms fluctuations for the aps conformation. The MSD deviations from these structures are 1.7 and 1.5 Å^2 for the ps F1.F2 and F3.F4 duplexes, respectively; and they are 0.86 and 0.84 Å^2 for F1.F4 and F2.F3 aps duplexes, respectively.

TABLE 3 Torsional angles for F2 in F1-F2 ps-DNA

Base	α	β	γ	δ	ϵ	ζ	χ
A1				138.5 (3.3)	182.7 (7.1)	267.4 (6.7)	250.8 (4.2)
A2	289.4 (9.3)	172.2 (9.1)	60.1 (8.6)	120.5 (12.8)	180.4 (9.0)	264.7 (12.2)	248.2 (12.8)
A3	292.2 (10.0)	171.0 (9.7)	61.3 (9.7)	119.7 (19.1)	206.0 (**42.2**)	232.7 (**49.8**)	244.9 (18.2)
A4	292.5 (11.4)	157.6 (**23.2**)	61.9 (10.1)	120.1 (**20.4**)	188.2 (**28.1**)	251.6 (**35.7**)	240.6 (17.5)
A5	294.7 (10.7)	166.5 (16.0)	65.3 (10.7)	127.4 (13.9)	177.5 (9.0)	263.2 (11.7)	242.2 (14.0)
T6	293.9 (10.6)	170.8 (9.9)	64.0 (10.2)	95.0 (21.9)	185.4 (**22.5**)	262.1 (**30.6**)	226.6 (16.1)
A7	294.6 (11.1)	171.8 (12.5)	64.9 (10.6)	137.4 (12.7)	188.3 (**25.0**)	251.2 (**33.2**)	255.1 (17.4)
A8	291.5 (10.7)	166.8 (15.5)	62.5 (9.9)	129.8 (12.4)	176.8 (8.8)	265.6 (11.0)	247.5 (12.9)
T9	295.3 (9.7)	170.2 (9.9)	66.3 (9.8)	129.0 (13.8)	258.9 (**38.8**)	169.3 (**45.0**)	239.9 (19.7)
T10	291.8 (11.9)	132.3 (**23.1**)	62.4 (9.0)	115.0 (21.4)	184.7 (8.7)	272.7 (13.7)	234.7 (19.2)
T11	286.9 (10.0)	169.4 (8.5)	59.8 (9.4)	85.6 (13.9)	181.1 (9.0)	278.0 (11.7)	221.5 (12.8)
A12	294.0 (9.7)	171.6 (8.4)	67.6 (9.9)	131.2 (13.3)	176.8 (8.8)	263.8 (11.0)	248.5 (13.1)
T13	293.0 (9.8)	170.6 (9.1)	63.4 (9.3)	90.6 (17.8)	186.6 (**30.1**)	258.1 (**37.8**)	222.6 (13.7)
A14	296.5 (10.8)	166.8 (14.9)	66.9 (9.9)	138.6 (10.5)	176.9 (7.3)	263.1 (9.5)	252.9 (11.7)
T15	299.1 (6.5)	171.7 (6.3)	59.5 (3.7)				247.2 (4.1)
Avg.	293 (11)	166 (17)	63 (10)	120 (23)	189 (30)	254 (37)	242 (18)

Time-averaged values of the dihedral angles (in degrees) for the sugar phosphate backbone (α, β, γ, δ, ϵ, ζ), and the glycosidic angle (χ) for the F2 oligomer when forming part of the F1-F2 ps DNA double helix. The SDs of the angles are given between parentheses under the corresponding averages. The bold-faced numbers indicate those angles for which the SDs are larger than the corresponding values for the same strand (F2), but in different conformation (aps DNA).

TABLE 4 Torsional angles for F2 in F2-F3 aps-DNA

Base	α	β	γ	δ	ϵ	ζ	χ
A1				134.6 (3.2)	181.2 (6.7)	268.2 (7.1)	249.8 (4.3)
A2	287.6 (9.2)	173.5 (8.9)	60.1 (9.1)	114.3 (13.5)	178.7 (8.5)	265.1 (11.6)	241.2 (12.9)
A3	293.3 (10.1)	171.8 (9.7)	62.9 (9.6)	118.0 (14.3)	178.4 (8.9)	263.8 (12.1)	238.9 (13.4)
A4	294.2 (9.8)	172.1 (9.7)	64.2 (9.5)	121.6 (13.8)	177.9 (8.9)	262.2 (12.6)	237.7 (13.1)
A5	294.5 (10.0)	173.1 (10.2)	64.6 (9.7)	122.9 (13.6)	178.7 (8.9)	261.6 (11.8)	235.6 (12.5)
T6	293.3 (10.2)	174.5 (9.8)	63.4 (9.2)	108.9 (17.2)	182.9 (9.1)	266.6 (13.9)	226.6 (14.4)
A7	291.6 (10.2)	172.7 (9.5)	62.5 (9.5)	127.6 (14.9)	178.8 (10.1)	261.2 (14.6)	245.3 (14.3)
A8	293.2 (10.0)	170.8 (10.2)	65.2 (9.6)	122.8 (13.7)	176.3 (9.2)	261.0 (12.3)	237.9 (12.3)
T9	295.6 (9.9)	173.3 (9.7)	65.8 (9.1)	117.6 (14.3)	179.5 (8.6)	264.0 (11.8)	228.7 (13.2)
T10	294.0 (10.2)	172.4 (9.6)	65.1 (9.3)	118.8 (14.6)	180.0 (8.2)	265.2 (11.0)	231.6 (14.7)
T11	292.3 (10.2)	172.4 (9.4)	63.3 (9.5)	113.9 (16.8)	181.0 (8.2)	267.9 (12.2)	232.6 (15.4)
A12	292.2 (10.0)	172.1 (9.5)	62.3 (9.3)	123.1 (13.8)	178.3 (8.6)	262.5 (11.6)	240.8 (13.2)
T13	292.6 (9.6)	172.9 (9.9)	63.5 (9.1)	104.2 (17.2)	181.9 (8.5)	269.8 (12.3)	225.1 (14.2)
A14	291.6 (9.9)	174.7 (8.8)	60.6 (8.7)	126.2 (12.5)	178.9 (7.7)	264.9 (9.8)	243.1 (11.8)
T15	294.2 (6.8)	172.2 (6.9)	60.7 (3.9)				234.0 (3.7)
Avg.	293 (10)	173 (9)	63 (9)	120 (16)	179 (9)	265 (12)	237 (14)

Table of time-averaged values of the dihedral angles (in degrees) for the sugar phosphate backbone (α, β, γ, δ, ϵ, ζ), and the glycosidic angle (χ) for the F2 oligomer when forming part of the F2-F3 aps DNA double helix. The SDs of the angles are given between parentheses under the corresponding averages.

(Berman et al., 1992) shows that for all thymine and adenine bases forming Watson-Crick A-T base pairs, the average dihedral angles are $\alpha = 305\ (\pm 37)$, $\beta = 172\ (\pm 22)$, $\gamma = 53\ (\pm 36)$, $\delta = 122\ (\pm 21)$, $\epsilon = 193\ (\pm 34)$, $\zeta = 250\ (\pm 38)$, and $\chi = 250\ (\pm 17)$ for thymine bases, and $\alpha = 302\ (\pm 43)$, $\beta = 171\ (\pm 27)$, $\gamma = 49\ (\pm 34)$, $\delta = 135\ (\pm 20)$, $\epsilon = 190\ (\pm 29)$, $\zeta = 252\ (\pm 36)$, and $\chi = 252\ (\pm 18)$ for adenine bases. With the exception of δ, all dihedral angles are similar to average angles of x-ray crystal structures' angles. The difference in the average value of δ comes from averaging over two conformations in a simulation, whereas x-ray structures are commonly fitted to the conformation with the largest occupancy.

The time-averaged structures of all four duplexes exhibit bifurcated hydrogen bonds along tracks of two or more consecutive A-T base pairs. These hydrogen bonds involve an attractive interaction between O2 (for aps) or O4 (for ps DNA) of T and N6 of A. Bifurcated (three center (Taylor, 1984)) hydrogen bonds in aps-DNA oligomers containing A-tracks in the sequence have been observed in crystal structures of DNA oligomers (Nelson et al., 1987; Coll et al., 1987) and protein DNA complexes (Mondragon and Harrison, 1991). Bifurcated hydrogen bonds consist of an arrangement in which a hydrogen atom forms contacts to two hydrogen bond acceptor atoms with the geometrical constraint that the bonds are in the *forward* direction (Taylor, 1984). That is, the donor-hydrogen-acceptor angle is $\geq 90°$. We accepted as a bifurcated hydrogen bond any configuration in which the angle between the donor-hydrogen-acceptor is $>90°$ and the distance between the donor and acceptor is <3.50 Å. This definition is markedly different from the commonly used definition of hydrogen for which the donor-hydrogen-acceptor angle is $>120°$ and the donor to acceptor distance is <3.2 Å. A survey of all DNA crystal structures exhibiting bifurcated hydrogen bonds (Leonard

et al., 1990, 1992; DiGabriele et al., 1989; Nelson et al., 1987; Coll et al., 1987; Mondragon and Harrison, 1991; Berman et al., 1992) shows that out of 24 observations, 11 contain angles between 90° and 95°, 5 contain angles between 95° and 100°, 3 contain angles between 100° and 105°, and 3 contain angles between 105° and 110°. The distances between donor to acceptor atoms vary from 2.80 to 3.8 Å. The angular distribution for DNA crystals is consistent with a similar distribution obtained by Taylor et al. (1984) using data from 889 organic crystal structures. The range of distances is much longer than what was considered by Taylor et al. as a three-center hydrogen bond.

For aps, bifurcated hydrogen bonds occur between 54 and 97% of the time with mean lifetimes ranging from 0.3 to 5.0 ps (only 19–39% of the configurations sampled satisfy the more stringent definition for hydrogen bonds). For ps, bifurcated hydrogen bonds occur less often, with occurrences ranging from 29 to 84% of the configurations and mean lifetimes ranging from 0.2 to 3.0 ps. The bases involved in bifurcated hydrogen bond in ps-DNA are different from those in aps-DNA. That is, in aps-DNA a bifurcated hydrogen bond is formed between T base in the *i*th Watson-Crick base pair, and an A base in the $i + 1$ WC base pair (labeling the T bases sequentially in the 5′ to 3′ direction). In ps-DNA, a bifurcated HB is formed between a T in the *i*th reverse WC base pair and an A base in the $i - 1$ reverse WC base pair. Notice that the direction of the hydrogen bond is the opposite of that in aps-DNA.

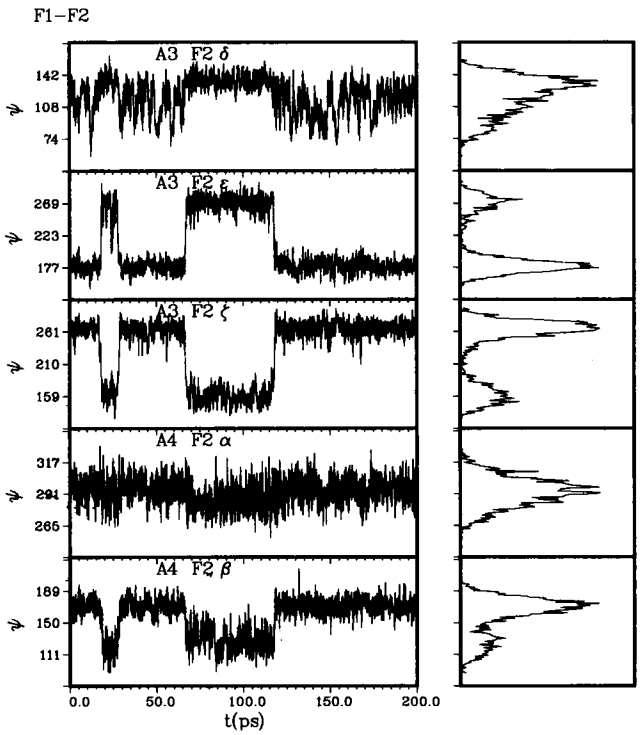

FIGURE 4 Plots of the time history (*left* curves) of the dihedral angles δ_j, ϵ_j, ζ_j, α_{j+1}, and β_{j+1}, in degrees, for A_3A_4 bases of F2 in the ps-DNA F1.F2 double helix. The right curves show histograms of the occurrence of a dihedral angle during the simulation, and are plotted on the l.h.s. curve. The distributions for the angles ϵ, ζ, and β are multi-modal. The distribution for δ is broad, but the history of the angles show frequent transitions from $\delta \approx 120°$ (C2′ endo sugar conformation) to $\delta \approx 80°$ (C3′ endo sugar conformation). These transitions are not easily distinguishable, unlike the transitions in ϵ, ζ, and β. Times are given in ps.

Dynamic behavior

Dihedral angle motions

Large variations in dihedral angles are a consequence of fast transitions between two (or more) conformations (Garcia, 1992, 1993a; Helfand 1983) where the system will show damped oscillations around each minimum. At nonregular intervals, a transition from one state to another will occur. These transitions involve the concerted motion of various connected dihedral angles. This is precisely the case for the oligomer studied here. Fig. 4 shows the time history during the simulation of the dihedral angles δ_i, ϵ_i, ζ_i, α_{i+1}, and β_{i+1}, where i is the base number in the chains' sequences, for the A_3 and A_4 bases of the F2 strand in the F1-F2 ps DNA-duplex. The left plots illustrate the time history of the dihedral angles, and the right plots show histograms of the occurrence of the dihedral angles. Notice that transitions in ϵ_i, ζ_i, and β_{i+1} are strongly correlated. That is, a transition in ϵ from t to g^+ occurs simultaneously with a transition of ζ from g^+ to t. Similarly, flips in β occur, but from t to just over the g^- barrier. Notice that the histograms for these angles are bimodal. Transitions from one conformation to another occur faster than 1 ps, whereas the mean residence time in the least populated conformation can be as long as 35 ps. The dihedral angle δ exhibits a broad distribution that covers both C2′-endo and C3′-endo sugar conformations. Transitions from one state to another occur frequently. This behavior is characteristic of a coupled nonlinear system. That is, the multimodal distributions cannot be described by normal mode analysis, and the correlation (or anticorrelations) between dihedral angle flip-flops is indicative of delocalized excitations.

As already mentioned above, the time history of some dihedral angles shows fast transitions from one minimum to another followed by damped oscillations around each of the minima. The transition from one state to another will occur at nonregular intervals. The average transition rate from one minimum to another can be obtained from a hazard analysis (Helfand, 1983) as described under Analysis of Dihedral Angle Transitions. The kinetics of the dihedral angle transitions was calculated for all angles δ and for the angles β, ϵ, and ζ highlighted in Tables 3 and 4. Table 5 lists the percentage of the time and the mean time of residence of the angles δ in two major conformations, C2′-endo and C3′-endo for the F2 oligomer in ps and aps conformations. Averages over all four single strands, the ratio of the percentage of the time spent in C2′-endo to the percentage of the time spent in C3′-endo conformations are: 45/55 and 70/30 for T in ps and aps duplexes, respectively; and 94/6 and 5/95 for

TABLE 5 Kinetics of torsional angles δ for F2 in F1-F2 ps-DNA and F2-F3 aps DNA

	F1-F2 ps DNA				F2-F3 aps DNA			
	C3′ endo		C2′ endo		C3′ endo		C2′ endo	
Base	%	τ	%	τ	%	τ	%	τ
A1	0	—	100	>200	0	—	100	>200
A2	5	0.5	95	13.1	13	0.6	87	5.6
A3	22	1.5	78	19.6	10	0.8	90	6.3
A4	18	1.7	82	5.6	5	0.5	95	16.7
A5	4	0.5	96	10.3	4	0.3	96	11.9
T6	74	7.8	2.6	2.9	37	0.9	63	1.8
A7	2	0.9	98	55.1	5	0.5	95	12.4
A8	0.5	0.4	99.5	46.5	4	0.5	95	8.7
T9	5	1.2	95	>200	10	0.5	90	4.9
T10	27	2.4	73	6.7	11	0.6	89	6.9
T11	92	8.8	8	0.8	19	0.9	81	3.3
A12	2	0.5	98	29.5	5	0.3	95	10.3
T13	84	34.2	16	18.6	53	1.3	47	1.0
A14	0.2	0.3	99.8	94.9	2	0.3	98	19.6
T15	0	—	100	>200	0	—	100	>200
Averages								
A	6		94		6		94	
T	56		44		26		74	

Percentage of the time and the mean time of residence (in ps), τ, of the angles δ in two major conformations, C2′-endo and C3′-endo for the F2 oligomers in ps and aps conformations. Transitions occur often with mean residence time in the minor conformation (when transitions occur) shorter than 2.6 picoseconds. On the average, T residues spend most of the time in the C3′-endo conformation in ps duplexes. The character of the transition between C2′-endo and C3′-endo is typical of disordered transitions.

A bases in ps and aps duplexes, respectively. Notice that, on the average, T residues spend most of the time in the C3′-endo conformation in ps duplexes. The transition between C2′-endo and C3′-endo are typical of disordered transitions. Notice that transitions occur often and that the mean residence time in the minor conformation (when transitions occur) is short (less than 2.6 ps). The mean residence time in the major conformations varies with the percent of residence in the major conformation from 1.5 (51%) to 50 (99%) ps. In interpreting the residence times, caution must be exerted. The potential error in the determination of these times will vary according to the ratio of the mean residence time to the total time of configurational averaging. We consider that in two instances the mean residence times have no statistical significance: 1) when the mean residence time is long (in general $\tau > t_{sampling}/2$ (Zwanzig, 1969); and 2) when the mean residence time of the complementary transition is longer than $t_{sampling}/2$.

The mean residence time and percentage of the time for two conformations for other sugar-backbone dihedral angles (β, ϵ, ζ) that exhibit transitions for all four strands in ps and aps conformations were also studied. These transitions are characteristic of *order-order* transitions. Most of these transitions describe collective motions in a time scale too long to be determined by our 200-ps simulations. For those transitions for which we were able to obtain significant statistics, the mean residence time in the major conformations are near 40 ps (for relative occupancies between 30/70 and 5/95). The mean residence time depends strongly on the occupancy ratio and is near 5 ps for minor populations between 5 and 12%, and is between 20 and 35 ps for minor populations between 12 and 30%.

Collective motions

To extract collective motions that best describe the fluctuations of the system, we employ the methodology described under Analysis of the MD Trajectories. This analysis consists in finding a set of directions in 3N dimensional space that best describe the MSD fluctuations of the system. Within this framework, a set of 3Nx3N matrices are diagonalized. The resulting eigenvalues are related to the mean-square displacements in the following way:

$$\langle x^2 \rangle = \frac{1}{N} \sum_{\alpha=1}^{3N} \lambda_\alpha, \tag{13}$$

where λ_α is the αth eigenvalue. Similarly, the eigenvector, ν_1, with the largest eigenvalue, λ_1, gives a direction that best describes the fluctuations of the system. Figs. 5 and 6 show the projections of the MD trajectories along the five directions corresponding to the largest eigenvalues, for ps and aps duplexes. Notice that for ps-DNA, one direction describes ≈30% of the fluctuations. These fluctuations are as large as the corresponding ms fluctuations for the whole aps-DNA molecule. The second largest fluctuation directions for the ps-DNA have eigenvalues similar to the largest eigenvalue direction of the aps-DNA molecules.

The motions described by the first vector correspond to a displacement of one strand, along the helix axis, relative to the other strand. That is, a displacement similar to the one described as a shearing mode by Prohofsky et al. (1982). The motion along the second vector represents a breathing motion where the grooves open and close. The amplitude of this mode is much larger than the amplitude of the corresponding

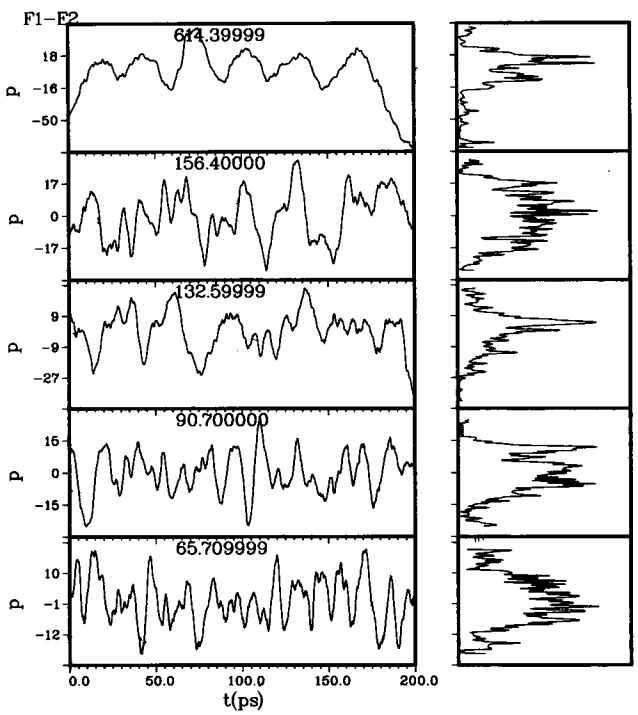

FIGURE 5 Time history of the projection of the MD trajectories along five directions that best describe the atomic fluctuations of the F1-F2 ps-DNA double helix during a 200 ps MD simulations at ≈300K. The number on top of each curve indicates the eigenvalue, in Å^2, corresponding to the given direction. Curves for decreasing eigenvalues are shown from top to bottom. The right curves show histograms of the occurrence of different projection values along the trajectory. The distribution for the first direction, $\lambda = 614.4$, is not unimodal. This direction describes 30% of the total atomic fluctuations. The first five directions describe 66% of the total fluctuations; the remaining 2863 directions describe the remaining 34% of the fluctuations. Times are given in ps.

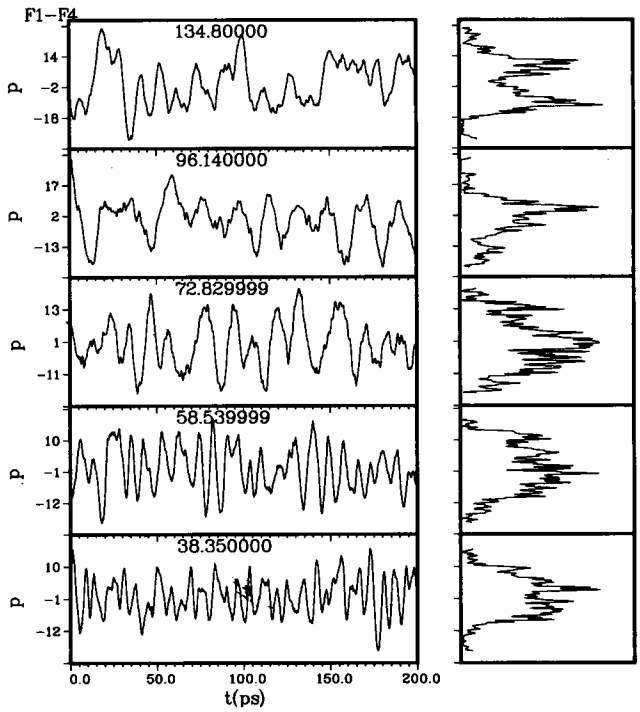

FIGURE 6 Similar plot as Fig. 4, but for the F1-F4 aps-DNA double helix. The eigenvalue of the first direction vector is much smaller than the corresponding value for the F1.F2 ps double helix. The distribution of the occurence of projection values along the first direction show two marked maxima. Transitions from one distribution to the other occur in a periodic fashion, not in an abrupt manner, as shown for the dihedral angles in Fig. 3.

mode in aps-DNA. Fig. 7 shows the MSD of the P atoms during the MD trajectory for F1-F2 ps-DNA, and the contribution to the fluctuations by each of the four directions that contribute the most to the fluctuations. The x axis represents the P atom number (P 1–14 for F1 and 15–28 for F2). The markers on the curves are: *filled circles* (λ_1, ν_1); *open circles* (λ_2, ν_2); *open squares* (λ_3, ν_3); *filled squares* (λ_4, ν_4). The total MSD for the P atoms show a maxima P_{21} on F2. There is another maxima around P_5 of F1. The largest eigenvalue vector describes an extended motion that involves both strands, with a maximum displacement occurring around P_6 and P_{21}. The second largest eigenvalue direction shows the largest displacement around P_{21}. Notice how the contribution to the MSD falls off with the mode number. That is, the first four modes contribute to a MSD of 1.03 Å^2, (i.e., 60% of the total fluctuations).

Energetics

The enthalpic contribution to the free energy arising from the duplexes' conformations and dynamics can be evaluated from the averaged potential energies of the duplexes. At constant temperature, this energy is given by the time average of the potential energy, $U(T) = \langle U_{tot}(T, t)\rangle_t$ (McQuarrie, 1975). Table 6 shows the resulting average energies and SDS. These calculations show that the aps duplexes are energetically favored over ps duplexes, in complete agreement with experimental data on two of these oligomers (F1-F2 (ps) and F1-F4 (aps)) and in contrast with previous molecular mechanics results, which suggested that ps-DNA would be more stable than aps-DNA (Pattabiraman, 1986). The differences in averaged energies for the four single-stranded oligomers in the ps and aps conformations is given by

$$\Delta E(\text{ps} \rightarrow \text{aps}) = E_{\text{aps}}(F1 - F4) + E_{\text{aps}}(F2 - F3) - E_{\text{ps}}(F1 - F2) - E_{\text{ps}}(F3 - F4). \quad (14)$$

The most significant terms contributing to the stability of aps oligomers over ps oligomers are the van der Waals and dihedral angle terms, indicating that the packing of the aps oligomers is better than the packing of the ps oligomers. The differences in torsional angle energy can be explained in terms of the larger flexibility of the ps oligomers. By sampling a larger configurational space as a result of transitions in dihedral angles from low-energy minima to high-energy minima, the molecule samples high-energy conformations during a significant fraction of time.

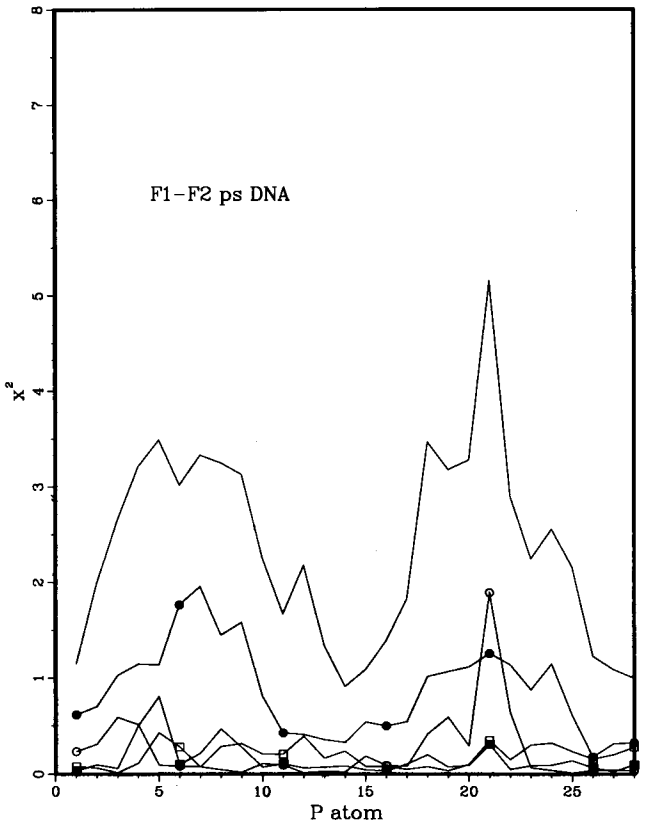

FIGURE 7 Mean square displacement, in Å^2, of *P*-atoms in the F1-F2 ps-DNA double helix. The curve without markers shows the ms fluctuations of the P-atoms during the MD simulation. The other curves show the ms fluctuations of the *P*-atoms along each of the four directions that best describe the atomic fluctuations during the simulation. The (●)-marked curve corresponds to the largest eigenvalue (λ_1 = 614.4 Å^2) direction (therefore, the single direction that describe most of the fluctuations); the (○)-marked curve corresponds to the second direction (λ_2 = 156 Å^2); the (□)-marked curve corresponds to the third direction (λ_3 = 133 Å^2); and the (■)-marked curve corresponds to the fourth direction (λ_4 = 91 Å^2). The contribution of each direction to the MSD is obtained by dividing the corresponding eigenvalue, λ_i, by the number of atoms, *N*.

From our calculations, we can obtain the differences in enthalpy between ps and aps double helices. These enthalpy differences cannot be directly measured by experiments. However, we can assume a hypothetical thermodynamic cycle where three states are considered.

1) A coil state containing the four-stranded oligomer.
2) The aps state containing the two aps double helices.
3) The ps state containing the two ps double helices.

If we neglect the interaction between duplexes and mixing effects, the transition from the duplexes to the single strands is studied by the helix coil transitions in solutions containing only ps or aps duplexes. (These assumptions are justified because near the helix coil transition temperature, the enthalpy does not depend strongly on temperature, salt concentration, and strand concentration. The dependence of melting temperatures on strand concentration is mainly due to the entropy of mixing.) The coil state (single strands) is the same in the two transitions:

$$F1.F2\ (\text{ps}) + F3.F4\ (\text{ps}) \rightarrow \text{coil}, \tag{15}$$

and

$$F1.F4\ (\text{aps}) + F2.F3\ (\text{aps}) \rightarrow \text{coil}, \tag{16}$$

irrespective of the strand orientation in the duplex. Therefore, the relative enthalpy difference in a hypothetical aps → ps transition can be obtained from measured values of the enthalpies in helix coil transitions and is given by

$$\Delta H_{\text{aps}\rightarrow\text{ps}} = \Delta H_{\text{F1.F2}} + \Delta H_{\text{F3.F4}} - \Delta H_{\text{F1.F4}} - \Delta H_{\text{F2.F3}}. \tag{17}$$

The same enthalpy difference can be obtained from our calculations,

$$\Delta H_{\text{aps}\rightarrow\text{ps}} = U_{\text{F1.F2}} + \Delta U_{\text{F3.F4}} - \Delta U_{\text{F1.F4}} - \Delta U_{\text{F2.F3}}. \tag{18}$$

The resulting enthalpies are listed in Table 7. The experimental values obtained from helix coil transitions are known for only two duplexes, F1.F2 (ps) DNA and F1.F4 (aps) DNA. However, analysis of melting data on a large set of ps- and aps-DNA oligomers by Rippe and Jovin (1989) yielded a set of parameters that allow, within a nearest neighbor stack model, estimation of the stability of ps and aps duplexes. The changes in enthalpy for all duplexes studied here are also given in Table 7. Notice that our results agree within 0.6 Kcal/mol, which is less than the accuracy of the enthalpies calculated using the nearest neighbor approximation. By calculating differences, we have eliminated absolute errors in the calculations. We would like to emphasize the fact that our calculations give the correct sign and magnitude of the relative stabilities (previous calculations comparing ps- and aps-DNA failed on both accounts), rather than the fact that the agreement is within 0.6 Kcal/mol.

The entropic contribution to the free energy resulting from atomic fluctuations can be computed, within the harmonic approximation, from the vibrational normal mode analysis of these oligomers (McQuarrie, 1975; Garcia, 1989a, b, 1993a). Instead of calculating the vibrational normal modes from the second derivative matrix evaluated at a local minimum of every duplex, for systems of this size we prefer to use the quasi-harmonic (Karplus, 1981; Levy, 1984; Brooks, 1988) approximation analysis of the trajectories at low (100 K) temperature. At low temperature, the distributions of fluctuations around the average configurations are unimodal and approximately described by Gaussian distributions. As already mentioned, this is a necessary requirement for the validity of the quasi-harmonic approximation. The calculated frequency spectra were used to calculate the vibrational free energies of the duplexes at 100 and 300 K. The low temperature frequency spectra were used to calculate the vibrational free energies at both temperatures. Fig. 8 shows the low frequency density of states and (low) frequency spectra for all four duplexes. Table 8 also

TABLE 6 Averaged energies (300K)

Duplex	E_P	E_{vdW}	E_{el}	E_{HB}	E_B	E_A	E_d
f1-f2 (ps)	944.8 (18.1)	−461.0 (5.5)	85.6 (0.9)	−15.0 (0.6)	352.2 (14.9)	432.4 (12.5)	375.1 (8.6)
f3-f4 (ps)	943.4 (18.1)	−459.9 (5.6)	85.2 (0.8)	−15.5 (0.6)	324.0 (16.7)	432.1 (17.0)	374.3 (8.9)
f1-f4 (aps)	924.1 (16.4)	−473.9 (5.9)	85.0 (0.6)	−14.4 (0.7)	328.2 (14.1)	436.6 (13.3)	357.9 (7.5)
f2-f3 (aps)	915.7 (16.3)	−474.7 (5.6)	85.1 (0.6)	−14.9 (0.6)	322.7 (3.7)	438.7 (12.1)	356.4 (7.3)
ΔE (ps → aps)	48.4	**27.7**	−0.3	−1.2	−1.7	−10.8	**34.1**

Average energies (in Kcal/mol) and SDs during the MD simulations at 300 K for each of the four duplexes. The last row lists the differences in energy between parallel and anti-parallel duplexes. The aps duplexes are energetically favored over ps duplexes, in complete agreement with experimental data on two of these oligomers (F1-F2 (ps) and F1-F4 (aps)). The difference in averaged energies for the four single-stranded oligomers in the ps and aps conformations is given by $\Delta E(\text{ps} \rightarrow \text{aps}) = E_{aps}(F1 - F4) + E_{aps}(F2 - F3) - E_{ps}(F1 - F2) - E_{ps}(F3 - F4)$. The terms that most significantly differ are the stacking (van der Waals) and torsional angle energies.

TABLE 7 Enthalpies (300K)

Duplex	$U_0 + H_{vib}$	$\Delta H_{exp}^{(fitted)}$	$\Delta H_{exp}^{(measured)}$
f1-f2 (ps)	1575.9	57.9	55.2
f3-f4 (ps)	1579.1	57.9	N.A.
f1-f4 (aps)	1545.5	85.0	78.8
f2-f3 (aps)	1550.3	89.2	N.A.
ΔH(aps − ps)	59.1	58.5	

Enthalpies (in Kcal/mol) obtained from calculations, from the nearest neighbor stacking model, and experiments for ps and aps DNA duplexes. U_0 is the time-averaged potential energy during the MD simulations. ΔH_{vib} is the harmonic enthalpic contribution calculated from quasi-harmonic analysis on MD trajectories. ΔH_{exp}^{fitted} is the fitted nearest neighbor stacking model enthalpies obtained by Rippe (1989). $\Delta H_{exp}^{(measured)}$ is the measured melting enthalpy differences. The last row shows the difference in enthalpy between ps and aps DNA duplexes obtained from the calculations and from the nearest neighbor model. Experimental data for the f3-f4 aps and f3-f3 ps duplexes are not available.

shows the vibrational free energy and enthalpy obtained from the quasi-harmonic analysis. Within the harmonic approximation, the contribution of local fluctuations to the free energy does not clearly discriminate between ps and aps duplexes. That is, if we rank the oligomers in order of stability as indicated by the vibrational free energy, A_{vib}, we get $F1 - F2$ (ps) > $F2 - F3$ (aps) > $F3 - F4$ (ps) > $F1$-$F4$ (aps). The differences in vibrational entropy are not sufficient to compensate for the differences in enthalpy. Similar relative stabilities are obtained from the vibrational free energy. The vibrational enthalpy does discriminate against ps-DNA, giving a lower enthalpy for aps-DNA than for ps. At room temperature (300 K), the mean-square fluctuations around equilibrium of ps oligomers are much larger than for aps oligomers. This will yield larger configurational entropy to the ps over aps oligomers. However, the quasi-harmonic approximation does not apply when multiple minima are sampled, as is the case at 300 K.

Considering previous normal mode calculations on various DNA (Garcia, 1993b) oligomers and the MSD displacements at 300 K, we can conclude that the order of flexibility of DNA in various conformations is

psDNA > aps(B)DNA > aps(A)DNA > aps(Z)DNA.

However, based on the quasi-harmonic results at low temperature (300 K), the order of flexibility would be

psDNA ~ aps(B)DNA > aps(A)DNA > aps(Z)DNA.

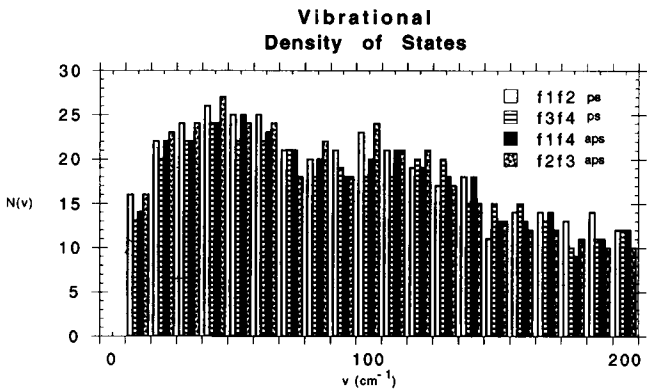

FIGURE 8 Low frequency density of states (dimensionless) (number of vibrational states within 10 cm^{-1} windows) for all four duplexes obtained from a quasi-harmonic analysis of the MD trajectories at 100K. Frequencies are given in cm^{-1}. Low frequency vibrational frequencies are mostly determined by collective, delocalized motions involving the whole molecule. High frequency vibrations (not shown here) are characteristic of localized motions involving displacements of a small number of atoms. Most of the atomic fluctuations from equilibrium and thermodynamics stability are determined (with the harmonic approximation) by low frequency modes. The spectra shown here show maxima near 50 and 100 cm^{-1}. The vibrational spectra for F1.F2 ps-DNA and F2.F3 aps-DNA exhibit the largest number of modes at the lowest frequencies (≈10 cm^{-1}). Notice from Table 8 that these two duplexes have the largest vibrational entropies.

TABLE 8 Vibrational free energies (300K)*

Duplex	U_0	A_{vib}	H_{vib}	TS_{vib}	$F = U_0 + A_{vib}$
f1-f2 (ps)	944.8	−830.1	631.1	1461.1	114.8
f3-f4 (ps)	943.4	−808.3	635.7	1444.0	135.1
f1-f4 (aps)	915.7	−814.8	629.8	1444.7	100.9
f2-f3 (aps)	924.0	−821.2	626.2	1448.1	102.2
ΔF(ps→aps)					46.8

* In Kcal.
Obtained from the quasi-harmonic analysis for all four duplexes.

At low temperatures, the fluctuations due to thermal excitations are not sufficient to permit flip-flop transitions of backbone torsional angles. Therefore, the local energy minima sampled by ps- and aps-DNA are very similar, as demonstrated by the quasi-harmonic analysis. At higher temperatures, flip-flop transitions of the backbone dihedral angles occur for both ps- and aps-DNA; however, due to the wider grooves in ps-DNA, transitions occur more easily, resulting in larger fluctuations.

CONCLUSIONS

Here we have used the MD simulation technique mainly as a convenient method to explore the conformational possibilities of the duplexes in the neighborhood of the averaged ps and aps structures. For this purpose, we think that is is sufficient to model the solvent very crudely (as a dielectric continuum) and limit the MD runs to 200 ps, a time reasonably long for observing the concerted motions described above, but not too demanding on computational resources. More realistic simulations of DNA, including water molecules, enough ions to emulate, e.g., a 0.1 M NaCl solution, and longer times are highly desirable, but not possible at present.

Fortunately, it is still possible to obtain very good quality information on ionic and specific hydration effects using a PMF approach (Soumpasis, 1984, 1989b; Klement, 1990; Hummer and Soumpasis, 1994). Such results concerning the salt dependence of the ps and aps conformational stabilities will be published elsewhere. Here, we have spent considerable effort to device techniques that could make the most out of the raw MD data and have described some of them above. These techniques have proven to be very useful for understanding subtle aspects of the conformational space sampling performed during the MD simulations.

The picture emerging from this work can be summarized as follows: in agreement with experimental results, the parallel-stranded form of DNA turns out to be thermodynamically less stable than the conformations of antiparallel-stranded B-family. Time-averaged ps structures are characterized by equally wide grooves, large twist angles, and rises (D_z) as well as low propeller twists. Dynamically, ps-DNA is much more flexible than the aps B-DNA. This finding, taken in conjunction with the results of previous work (Garcia, 1993b) that showed that the aps B-form is more flexible than the A- and Z-DNA, means that ps-DNA is the most flexible DNA double-stranded conformation known to date. This enhanced flexibility may have important consequences for the reactivity of ps-DNA in intercalation and other binding equilibria.

The wide grooves of ps-DNA allow for pronounced correlated, nonlinear, flip-flop motions of the backbone angles involving *P*-atoms. This type of motion may be the cause for the multiple *P*-NMR resonances observed in ps-DNA.

Collective motions are responsible for most of the fluctuations. That is, the atomic fluctuations are not well described by large fluctuations of individual atoms of small groups of atoms, but by concerted motions of various atoms. These modes are nonlinear in the sense that they involve transitions between states, and the distribution of the displacements along these modes are multi-modal. The mean time between transitions for the largest displacement modes is around 50 ps. Normal mode analysis give modes with characteristic periods around 5 ps. Molecular dynamics simulations of proteins (e.g., BPTI) (Levitt and Sharon, 1988; Levitt, 1990) in solution and in vacuum have shown that the atomic fluctuations (as measured by the MSD) are larger for systems simulated in vacuum than for identical systems simulated in aqueous solution. Similar results are expected for DNA oligomers. However, dihedral angle transitions are observed more often for systems in solution than for systems in vacuum (A. E. Garcia, unpublished results).

We wish to thank our colleagues D. Gray, G. Gupta, J. A. Krumhansl, V. Kuryari, K. Rippe, and C. S. Tung for many valuable discussions.
This work was supported by the U. S. Department of Energy. D. M. Soumpasis acknowledges support of this work by the Bundeministerium fur Forschung und Technologie, Germany.

REFERENCES

Arnott, S., P. Campbell-Smith, and P. Chandrasekaran. 1976. CRC Handbook of Biochemistry. Vol. 2. CRC Press, Boca Raton, FL. 411–422.

Berendsen, H. J. C., J. P. M. Postma, W. F. van Gunsteren, and J. R. Kaak. 1984. Molecular Dynamics with coupling to an external bath. *J. Chem. Phys.* 81:3654–3690.

Berman, H. M., W. K. Olson, D. L. Beveridge, J. Westbrook, A. Gelbin, T. Demeny, S-H. Hsieh, A. R. Srinivasan, and B. Schneider. 1992. The nucleic acid database: a comprehensive relational database of three dimensional structures of nucleic acids. *Biophys. J.* 63: 751–759.

Brooks, C. L., M. Karplus, M. B. Montgomery-Pettitt. 1988. Proteins: A Theoretical Perspective of Dynamics, Structure, and Thermodynamics. Advances in Chemical Physics. Vol. LXXI. John Wiley & Sons, New York. 259 pp.

Catasti, P., G. Gupta, A. E. Garcia, R. Ratliff, L. Hong, P. Yau, R. K. Moyziz, and E. M. Bradburry. 1994. Unusual Structures of the tandem repetitive DNA sequences located at the human centromeres. *Biochemistry.* 33:3819–3830.

Coll, M., C. A. Frederick, A. H-J. Wang, and A. Rich. 1987. A bifurcated hydrogen-bonded conformation in the d(A. T) base pairs of the DNA dodecamer d(CGCAAATTTGCG) and its complex with distamycin. *Proc. Natl. Acad. Sci. USA.* 84:8385–8389.

DiGabriele, A. D., M. R. Sanserson, and T. A. Steitz. 1989. The conformational variability of an adenosine.ionosine base-pair in a synthetic DNA dodecamer. *Proc. Natl. Acad. Sci. USA.* 86:1816–1820.

García, A. E. 1992. Non-linear dynamics of proteins. *Phys. Rev. Lett.* 68: 2696–2699.

García, A. E. 1993. Harmonic and anharmonic dynamics of DNA oligomers. *In* Computation of Biomolecular Structures—Achievements, Problems and Perspectives. D. M. Soumpasis and T. M. Jovin, editors. Springer Verlag, Berlin. 165–199.

Garcia, A. E., G. Gupta, D. M. Soumpasis, and C. S. Tung. 1990. Energetics of the hairpin to mismatched duplex transition of d(GCCGCAGC) in NaCl solution. *J. Biomol. Struct. Dyn.* 8:173–186.

Garcia, A. E., and J. A. Krumhansl. 1989. Role of the Coulomb interaction in the low-frequency density of states of DNA double helices. *Phys. Rev.* A37:4875–4878.

García, A. E., and D. M. Soumpasis. 1989. Harmonic vibrations and thermodynamic stability of a DNA oligomer in monovalent salt solution. *Proc. Natl. Acad. Sci. USA.* 86:3160–3164.

García, A. E., and L. Stiller. 1993. Computation of the mean residence time of water in the hydration shells of biomolecules. *J. Comp. Chem.* 14: 1396–1406.

Germann, M. W., B. W. Kalisch, and J. H. van de Sande. 1988. Relative stability of parallel- and antiparallel-stranded duplex DNA. *Biochemistry.* 27:8302–8306.

Germann, M. W., H. J. Vogel, R. T. Pon, and J. H. van de Sande. 1989. Characterization of a parallel-stranded DNA hairpin. *Biochemistry.* 28: 6220–6228.

Grady, D. I., R. L. Ratliff, D. L. Robinson, E. C. McCanlies, J. Meyne, and R. K. Moyziz. 1992. Highly conserved repetitive DNA sequences are present at human centromeres. *Proc. Natl. Acad. Sci. USA.* 89: 1695–1699.

Gupta, G., M. Bansal, and V. Sasisekharan. 1980. Conformational flexibility of DNA: Polymorphism and handeness. *Proc. Natl. Acad. Sci. USA.* 77: 6486–6490.

Helfand, E.. 1983. Brownian dynamics simulation of system with transitions, particularly conformational transitions in chain molecules. *Physica.* 118A:123–135.

Hobza, P., and C. Sandorfy. 1987. Nonempirical calculations on all the possible 29 possible DNA base pairs. *J. Am. Chem. Soc.* 109:1302–1307.

Il'ichova, I. A., Y. P. Lysov, A. A. Chernyi, A. K. Schyolkina, B. P. Gottikh, and V. L. Florentiev. 1990. Parallel double helices of DNA conformational analysis of regular helices with 2nd order symmetry axis. *J. Biomol. Struct. Dyn.* 7:879–897.

Jovin, T. M., K. Rippe, N. B. Ramsing, R. Klement, W. Elhorst, and M. Vojtiskova. 1990. Parallel stranded DNA. *In* Structure and Methods, Volume 3: DNA RNA. R. H. Sarma and M. H. Sarma, editors. Adenine Press, Guilamine, NY. 155–174.

Karplus, M., and J. N. Kushick. 1981. Method for estimating the configurational entropy of macromolecules. *Macromolecules.* 14:325–332.

Klement R., D. M. Soumpasis, E. V. Kitzing, and T. M. Jovin. 1990. Inclusion of ionic interactions in force field calculations of charged biomolecules: DNA structural transitions. *Biopolymers.* 29:1089–1103.

Klysik J., K. Rippe, and T. M. Jovin. 1990. Reactivity of parallel stranded DNA to chemical modification reagents. *Biochemistry.* 29: 9831–9839.

Klysik J, K. Rippe K, and T. M. Jovin. 1991. Parallel-stranded DNA under topological stress- rearrangement of $(dA)_{15}$. $(dT)_{15}$ to d(AAT) triplex. *Nucleic Acids Res.* 19:7145–7154.

Krumhansl, J. A. 1985. Anharmonicity in computer studies of biopolymers. *In* Computer Analysis for Life Science. C. Kawabata and A. R. Bishop, editors. Ohmsha LTD, Tokyo. 78–88.

Lankhorst, P. P., C. A. G. Haasnoot, C. Erkelens, C., and C. Altona. 1984. Carbon-13 NMR in conformational analysis of nucleic acid fragments. 2. A reparametrization of the Karplus equation for vicinal NMR coupling constants in CCOP and HCOP fragments. *J. Biomol. Struct. Dyn.* 1:1387–1405.

Lee, J. S. 1990. The stability of polypurine tetraplexes in the presence of mono and divalent cations. *Nucleic Acids Res.* 18:6057–6060.

Lee, J. S., D. H. Evans, and A. R. Morgan. 1980. Polypurine DNAs and RNAs form secondary structures which may be tetra-stranded. *Nucleic Acids Res.* 8:4305–4326.

Lee, J. S., D. A. Johnson, and A. R. Morgan. 1979. Complexes formed by $(pyrimidine)_n$. $(purine)_n$ DNAs on lowering pH are 3-stranded. *Nucleic Acids Res.* 6:3073–3091.

Leonard, G. A., E. D. Booth, W. N. Hunter, and T. Brown. 1992. The conformational variability of an adenosine ionosine base-pair in a synthetic DNA dodecamer. *Nucleic Acids Res.* 20:4753–4759.

Leonard, G. A., J. Thomson, W. P. Watson, and T. Brown. 1990. High resolution structure of a mutagenic lesion in DNA. *Proc. Natl. Acad. Sci. USA.* 87:9573–9576.

Levitt, M. 1989. Molecular dynamics of macromolecules in water. *Chemica Scripta.* 29A:197–203.

Levitt, M., and R. Sharon. 1988. Accurate simulation of protein dynamics. *Proc. Natl. Acad. Sci. USA.* 85:7557–7561.

Levy, R. M., M. Karplus, J. N. Kushick, and D. Perahia. 1984. Evaluation of the configurational entropy for proteins: application to molecular dynamics simulations of an α-helix. *Macromolecules.* 17:1370–1374.

Lu, M., Q. Guo, and N. R. Kallenbach. 1992. Thermodynamics of G-tetraplex formation by telomeric DNA. *Biochemistry.* 31: 2455–2459.

McLachalan, J. 1979. Least square fitting of two structures. Appendix in Gene duplication in the structural evolution of chymotrypsin. *J. Mol. Biol.* 128:49–79.

McQuarrie, D. 1976. Statistical Mechanics. Harper & Row, New York. 641 pp.

Mei, W. N., M. Kohli, E. W. Prohofsky and L. L. van Zandt. 1981. Acoustic modes and non-bonded interactions of the double helix. *Biopolymers.* 20:833–852.

Mondragon, A., and S. C. Harrison. 1991. The pahge-434 CRO/OR1 complex at 2.5 Å resolution. *J. Mol. Biol.* 219:321–334.

Nelson, H. C. M., J. T. Finch, B. F. Luisi, and A. Klug. 1987. The structure of an oligo(dA).oligo(dT) track and its biological implications. *Nature.* 330:221–226.

Otto, C., G. A. Thomas, K. Rippe, T. M. Jovin, and W. L. Pelicolas. 1991. The hydrogen-bonding structure in parallel-stranded duplex DNA is reverse Watson-Crick. *Biochemistry.* 30:3062–3069.

Pattabiraman, N. 1986. Can the double helix be parallel? *Biopolymers.* 25: 1603–1606.

Pearlman, D. A., D. A. Case, J. C. Caldwell, G. L. Siebel, U. C. Singh, P. Weiner, and P. A. Kollman. 1991. AMBER 4.0. University of California, San Francisco.

Powers, R., R. K. Olsen, and D. G. Gorenstein. 1989. 2-dimensional H^1 and P^{31} NMR spectra of a decamer oligodeoxiribonucleotide duplex and a Quinolaxine tandem drug duplex complex. *J. Biomol. Struct. Dyn.* 7: 515–556.

Powers, R., C. R. Jones, and D. G. Gorenstein. 1990. 2-dimensional H^1 and P^{31} NMR spectra and restrained molecular dynamics structure on oligodeoxiribonucleotide duplex refined via a hybrid relaxation matrix procedure. *J. Biomol. Struct. Dyn.* 8:253–294.

Ramsing, N. B., and T. M. Jovin. 1988. Parallel stranded duplex DNA. *Nucleic Acids Res.* 16:6659–6676.

Ramsing, N. B., K. Rippe, and T. M. Jovin. 1989. Helix-coil transition of parallel stranded DNA—Thermodynamics of hairpin and linear duplex oligonucleotides. *Biochemistry.* 28:9528–9535.

Rentzeperis, D., K. Rippe, T. M. Jovin, and L. A. Marky. 1992. Calorimetric characterization of parallel-stranded DNA stability. conformational flexibility and ion binding. *J. Amer. Chem. Soc.* 114: 5926–5928.

Rippe K., V. Fritsch, E. Westhof, and T. M. Jovin. 1992. Alternating d(g-A) sequences form parallel-stranded DNA homoduplexes. *EMBO J.* 11:3777–3786.

Rippe, K., and T. M. Jovin. 1989. Substrate properties of 25 NT parallel-stranded linear duplexes.. *Biochemistry.* 28:9542–9549.

Rippe, K., N. B. Ramsing, and T. M. Jovin. 1989. Spectroscopic properties and helical stabilities of 25 nt parallel-stranded linear DNA duplexes. *Biochemistry.* 28:9536–9541.

Rippe, K., N. B. Ramsing, R. Klement, and T. M. Jovin. 1990. A parallel-stranded linear DNA duplex incorporating dC.dG base pairs. *J. Biomol. Struct. Dyn.* 7:1199–1209.

Robinson, H., G. A. Van der Mare, J. H. Van Boom, and A. H.-J. Wang. 1992. Unusual DNA conformation at low pH revealed by NMR-parallel-stranded duplex with homo base pairs. *Biochemistry.* 31:10510–10517.

Robinson, H., and A. H.-J. Wang. 1993. 5'-CGA sequence is a strong motif for homo base-paired parallel stranded duplex as revealed by NMR analysis. *Proc. Natl. Acad. Sci. USA.* 90:5224–5228.

Saenger, W. 1984. Principles of Nucleic Acid Structure. Springer Verlag, New York.

Soumpasis, D. M. 1984. Statistical mechanics of the B-Z transition of DNA: contribution of diffuse ionic interactions. *Proc. Natl. Acad. Sci. USA.* 81:5116–5120.

Soumpasis, D. M., A. E. García, R. Klement, and T. M. Jovin. 1990. The Potentials of mean force (PMF) approach for treating ionic effects on biomolecular structures in solution. *In* Theoretical Biochemistry and Molecular Biophysics. D. L. Beveridge and R. Lavery, editors. Adenine Press, Guillermine, NY. 343–360.

Soumpasis, D. M., and C. S. Tung. 1988. A rigorous basepair oriented description of DNA structures. *J. Biomol. Struct. Dyn.* 6:397–420.

Soumpasis, D. M., C. S. Tung, A. E. Garcia. 1991. Rigorous description of DNA structures. 2- On the computation of best axes, planesand helices from atomic coordinates. *J. Biomol. Struct. Dyn.* 8: 867–888.

Taylor, R., O. Kennard, and W. Versichel. 1984. Geometry of the N—H· · ·O=C hydrogen bond. 2. Three-center ("Bifurcated") and four-center ("trifurcated") bonds. *J. Am. Chem. Soc.* 106: 244–248.

van de Sande, J. H., N. B. Ramsing, M. W. Germann, W. Elhorst, B. W. Kalisch, E. von Kizing, R. T. Pon, R. C. Clegg, and T. M. Jovin. Parallel stranded DNA. *Science*. 241:551–557.

van Gunsteren, W. F., and H. J. C. Berendsen. 1977. Algorithms for macromolecular dynamics and constraint dynamics. *Mol. Phys.* 34: 1311–647.

van Gunsteren, W. F., H. J. C. Berendsen, R. G. Geurtsen, and H. R. J. Zwinderman. 1986. A molecular dynamics computer simulation of an eight-base-pair DNA fragment in aqueous solution: Comparison with experimental two-dimensional NMR data. *Ann. N. Y. Acad. Sci.* 482: 287–303.

Weiner, S. C., P. A. Kollman, D. A. Case, U. C. Singh, C. Ghio, G. Alagona, S. Profeta, and P. Wiener. 1984. A new force field for molecular mechanical simulations of nucleic acids and proteins. *J. Am. Chem. Soc.* 106:765–784.

Weiner, S. C., P. A. Kollman, D. T. Nguyen, and D. A. Case. 1986. An all atom force field for simulations of proteins and nucleic acids. *J. Comp. Chem.* 7:230–252.

Zhow, N., M. W. Germann, J. H. van de Sande, N. Pattabiraman, and H. J. Vogel. 1993. Solution structure of the parallel-stranded hairpin $d(T_8/C_4A_8)$ as determined by 2-dimensional NMR. *Biochemistry*. 32: 646–656.

Zwanzig, R., and N. K. Ailawadi. 1969. Statistical error due to finite time averaging in computer experiments. *Phys. Rev.* 182:280–283.